Appl. Phys. B 72, 691–696 (2001) / Digital Object Identifier (DOI) 10.1007/s003400100553

Applied Physics B
Lasers
and Optics

Anisotropic self-diffraction under Bragg mismatching

B. Wang[1], C.-C. Sun[1,*], T.-H. Yang[2], P. Ye[3], J.-Y. Chang[1]

[1] Institute of Optical Sciences, National Central University, Chung-Li 320, Taiwan
[2] Institute of Electro-Optical Engineering, National Chiao Tung University, Hsinchu, Taiwan
[3] Institute of Physics, Chinese Academy of Sciences, Beijing, P.R. China

Received: 11 July 2000/Revised version: 2 January 2001/Published online: 30 March 2001 – © Springer-Verlag 2001

Abstract. Anisotropic self-diffraction (ASD) under Bragg mismatch has been studied. We derive a solution that can describe well the diffraction characteristics of the anisotropic self-diffraction under Bragg mismatch. The solution is useful for estimating the Bragg constraint when the ASD is applied to optical information processing. Both the theory and the experiment are presented.

PACS: 42.40.My; 42.40.Pa

Photorefractive materials have been extensively applied to many applications, including phase conjugation, optical information processing, and optical sensing, owing to their real-time hologram characteristic [1, 2]. $BaTiO_3$ is one of the most important photorefractive crystals for its large response in refractive index change. The response of the refractive index change depends on the incident configuration, including polarization, incident angle, grating period and crystal orientation. To obtain a large refractive index change in $BaTiO_3$, Fainman et al. [3] proposed that a special-cut configuration for the optic axis lying on the incident plane can perform large gain in two-beam coupling, and Hong et al. [4] demonstrated a strong volume hologram with use a special-cut crystal. On the other hand, Sun et al. proposed and demonstrated a strong volume hologram with the use of a normal-cut configuration for the optic axis normal to the incident plane [5, 6]. The incident condition of the latter case is called anisotropic diffraction, where the large modulation exists only between the ordinary and extraordinary rays and the refractive index change could be as high as 2×10^{-4} in $BaTiO_3$. A special incident configuration of anisotropic diffraction condition is anisotropic self-diffraction (ASD), in which no extra reading beam is required. The incident beams act not only as the writing beams, but also as the reading beams so that the diffraction efficiency can not be described by Kogelnik's formula [7]. The diffraction formula for the ASD under Bragg match has been proposed by Kukhtarev et al. [8]. Based on the ASD in $BaTiO_3$, many applications have been proposed, including matrix–matrix multiplication and digital logic operation owing to the cross-interaction between the writing and diffraction beams [9, 10], incoherent-to-coherent conversion owing to the high diffraction efficiency in $BaTiO_3$ [11], and symmetry filtering owing to the inherent auto-convolution characteristic [12]. One of the most important parameters for optical information processing based on a volume hologram is the Bragg constraint. However, the limitation of the image/signal processing is unclear because the diffraction under Bragg mismatch is not well understood. Although the Bragg constraint of the ASD can be obtained through numerical methods, a simple formula for estimating the Bragg constraint and the shift tolerance of an optical information processor is preferred. In this paper, we demonstrate the ASD under Bragg mismatch in theory and experiment. In the following, we briefly review the theory of the ASD under phase match. In Sect. 2, we derive a solution of the coupled equations in an approximation of small modulation strength, and then we obtain a quasi-general solution of the coupled equations. The corresponding experimental results in $BaTiO_3$ are presented in Sect. 3.

1 ASD under phase match

Figure 1 shows the schematic diagram of the ASD in k space. The optic axis is perpendicular to the incident plane. Let $\boldsymbol{K}_{e1}$ and $\boldsymbol{K}_{e2}$ be wave vectors of the two writing beams with extraordinary polarization, and $\boldsymbol{K}_{o1}$ and $\boldsymbol{K}_{o2}$ be wave vectors of the diffracted beams with ordinary polarization. $\boldsymbol{K}_g$ is the grating vector defined as

$$\boldsymbol{K}_g = \boldsymbol{K}_{e2} - \boldsymbol{K}_{e1}. \tag{1}$$

Thus, the Bragg conditions of the ASD are written as

$$\boldsymbol{K}_{o1,2} = \boldsymbol{K}_{e1,2} \mp \boldsymbol{K}_g. \tag{2}$$

*Corresponding author.
(Fax: +886-3/425-2897, E-mail: ccsun@ios.ncu.edu.tw)

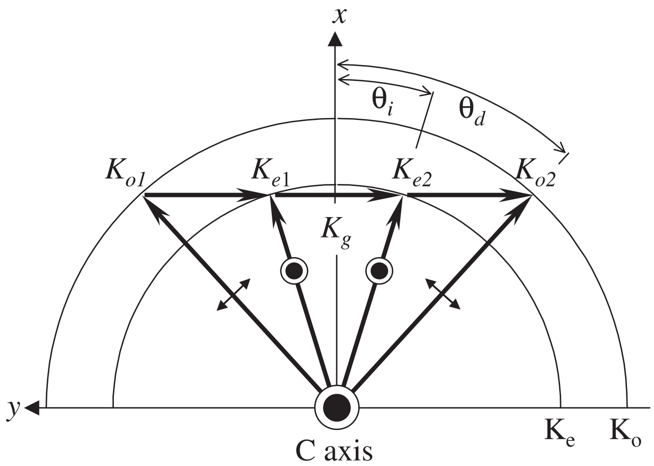

Fig. 1. Schematic diagram of the ASD in k space

According to (1) and (2), we can express the relation between the writing and the diffraction angles as

$$\begin{aligned} K_{\mathrm{e}} \cos \theta_{\mathrm{i}} &= K_{\mathrm{o}} \cos \theta_{\mathrm{d}}, \\ 3K_{\mathrm{e}} \sin \theta_{\mathrm{i}} &= K_{\mathrm{o}} \sin \theta_{\mathrm{d}}, \end{aligned} \tag{3}$$

or,

$$\begin{aligned} \theta_{\mathrm{i}} &= \sin^{-1}\left[\frac{1}{n_{\mathrm{e}}}\left(\frac{n_{\mathrm{o}}^2 - n_{\mathrm{e}}^2}{8}\right)^{1/2}\right] \\ \theta_{\mathrm{d}} &= \sin^{-1}\left[\frac{3}{n_{\mathrm{o}}}\left(\frac{n_{\mathrm{o}}^2 - n_{\mathrm{e}}^2}{8}\right)^{1/2}\right], \end{aligned} \tag{4}$$

where θ_{i} and θ_{d} are the writing and the diffraction angles, respectively; n_{e} and n_{o} are the extraordinary and ordinary refractive index, respectively. The coupled equations of the ASD under phase match can be expressed as [8]

$$\begin{aligned} \frac{\partial A_{\mathrm{e}1,2}}{\partial x} &= \mp\gamma \frac{A_{\mathrm{e}1,2}^{*} A_{\mathrm{e}2,1}}{I_0} A_{\mathrm{o}1,2} \\ \frac{\partial A_{\mathrm{o}1,2}}{\partial x} &= \pm\gamma \frac{A_{\mathrm{e}1,2} A_{\mathrm{e}2,1}^{*}}{I_0} A_{\mathrm{e}1,2}, \end{aligned} \tag{5}$$

where the A's are complex amplitudes, $I_0 = |A_{\mathrm{e}1}(0)|^2 + |A_{\mathrm{e}2}(0)|^2$, $\gamma = \frac{\pi \Delta n}{\lambda}$, λ is the wavelength in the vacuum, and Δn is the refractive index change. From (5) obviously it is shown that the coupling exists only between the extraordinary and ordinary waves. It is owing to the zero diagonal elements of the coupling tensor of $BaTiO_3$ when the optical axis is normal to the incident plane [13, 14]. This means that the coupling of those beams with the same polarizations (i.e. e–e and o–o) is inhibited. Although a weak coupling can take place through the photogalvanic effect [15], efficient coupling happens only in the anisotropic cases, i.e. the o–e coupling. Let the complex amplitudes be expressed as

$$\begin{aligned} A_{\mathrm{e}1,2} &= \sqrt{I_{\mathrm{e}1,2}} \exp\left(\mathrm{i}\Psi_{\mathrm{e}1,2}\right), \\ A_{\mathrm{o}1,2} &= \sqrt{I_{\mathrm{o}1,2}} \exp\left(\mathrm{i}\Psi_{\mathrm{o}1,2}\right) \end{aligned} \tag{6}$$

where the I's are the intensities and Ψ's are the phases. Substituting (6) into (5) and using the conversation laws [8]

$$\begin{aligned} I_{\mathrm{e}1,2}(x) + I_{\mathrm{o}1,2}(x) &= I_{\mathrm{e}1,2}(0) \\ (I_{\mathrm{e}1} I_{\mathrm{o}2})^{1/2} - (I_{\mathrm{e}2} I_{\mathrm{o}1})^{1/2} &= 0, \end{aligned} \tag{7}$$

we can obtain the solutions of (5) as [8]

$$\begin{aligned} I_{\mathrm{e}1,2}(x) &= \frac{I_{\mathrm{e}1,2}(0)}{1 + (\gamma m x)^2} \\ I_{\mathrm{o}1,2}(x) &= \frac{I_{\mathrm{e}1,2}(0)}{1 + (\gamma m x)^{-2}}, \end{aligned} \tag{8}$$

and

$$\Psi_{\mathrm{o}1,2} = 2\Psi_{\mathrm{e}1,2} - \Psi_{\mathrm{e}2,1}, \tag{9}$$

where m is the modulation depth of the optical interference gratings. From (8) we can find that the writing beams $I_{\mathrm{e}1,2}$ also work as the reading beams, and the diffraction efficiency does not oscillate as the crystal thickness increases like the traditional transmission volume gratings. So the behavior of the ASD is different from that described by Kogelnik's formula.

2 ASD under phase mismatch

The schematic diagram of the ASD under Bragg mismatch is shown in Fig. 2. We define the wave vectors as

$$\begin{aligned} \boldsymbol{K}_{\mathrm{e}1,2} &= \alpha_{\mathrm{e}1,2}\boldsymbol{x} + \beta_{\mathrm{e}1,2}\boldsymbol{y}, \\ \boldsymbol{K}_{\mathrm{o}1,2} &= \alpha_{\mathrm{o}1,2}\boldsymbol{x} + \beta_{\mathrm{o}1,2}\boldsymbol{y}, \end{aligned} \tag{10}$$

where $\boldsymbol{x}$ and $\boldsymbol{y}$ are unit vectors. The relations between the wave vectors and the grating vector can be expressed as

$$\boldsymbol{K}_{\mathrm{g}} = \beta_{\mathrm{e}2} - \beta_{\mathrm{e}1} = \beta_{\mathrm{o}2} - \beta_{\mathrm{e}2} = \beta_{\mathrm{e}1} - \beta_{\mathrm{o}1}. \tag{11}$$

The phase mismatch can be written as

$$\Delta\alpha = \alpha_{\mathrm{o}1} - \alpha_{\mathrm{e}1} = \alpha_{\mathrm{o}2} - \alpha_{\mathrm{e}2}, \tag{12}$$

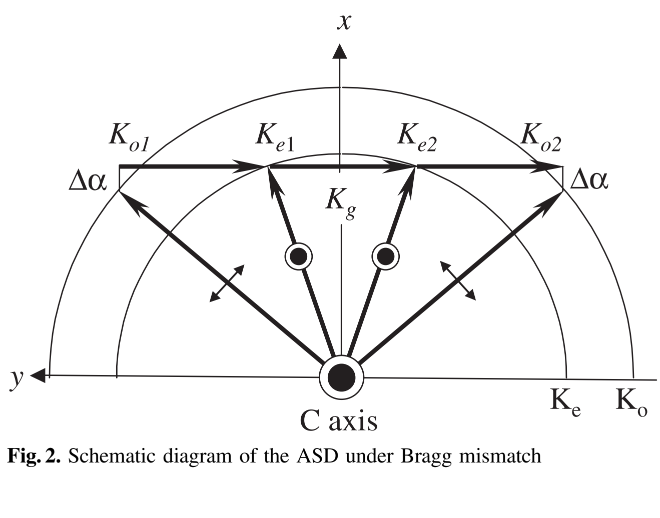

Fig. 2. Schematic diagram of the ASD under Bragg mismatch

where $\Delta\alpha$ is the quantity of phase mismatch when the incident angle is deviated from the Bragg angle. According to (10)–(12), the coupled equations expressed in (5) can be rewritten as

$$\frac{\partial A_{e1,2}}{\partial x} = \mp\gamma \frac{A^*_{e1,2}A_{e2,1}}{I_0} A_{o1,2}\exp(-i\Delta\alpha x)$$
$$\frac{\partial A_{o1,2}}{\partial x} = \pm\gamma \frac{A_{e1,2}A^*_{e2,1}}{I_0} A_{e1,2}\exp(-i\Delta\alpha x). \tag{13}$$

We first solve the coupled equations under an approximate condition. Now we consider (13) under the condition of small modulation, i.e. low diffraction efficiency. In this condition, we can let the variation of the incident extraordinary beams be infinitesimal and define the following equations,

$$\frac{dA_{e1}}{dx} = \frac{dA_{e2}}{dx} = 0. \tag{14}$$

Substituting (14) into (13), we can obtain the solutions of (13) under small modulation as

$$A_{e1,2}(x) = A_{e1,2}(0)$$
$$A_{o1,2}(x) = \gamma \frac{A^2_{e1,2}A^*_{e2,1}}{I_0}\frac{\exp(i\Delta\alpha x)-1}{i\Delta\alpha}. \tag{15}$$

Then substituting (6) into (15), we have the solutions expressed as follows,

$$I_{e1,2}(x) = I_{e1,2}(0)$$
$$I_{o1,2}(x) = I_{e1,2}(0)\left[\gamma m\frac{\sin(\Delta\alpha x/2)}{\Delta\alpha/2}\right]^2, \tag{16}$$

and

$$2\Psi_{e1,2} - \Psi_{e2,1} - \Psi_{o1,2} = -\frac{\Delta\alpha}{2}x. \tag{17}$$

As shown in (17), we find that the phase relation under Bragg mismatch is different from that under Bragg match as shown in (9).
To derive the solutions of the general case, we substitute (6) into (13). Then the coupled equations of the ASD under Bragg mismatch can be expressed as

$$\frac{1}{2(I_{e1,2})^{1/2}}\frac{\partial I_{e1,2}}{\partial x} = \mp\gamma\frac{(I_{e1}I_{e2})^{1/2}}{I_0}(I_{o1,2})^{1/2} \times\cos(\Psi_{o1,2} - 2\Psi_{e1,2} + \Psi_{e2,1} - \Delta\alpha x)$$
$$\frac{1}{2(I_{o1,2})^{1/2}}\frac{\partial I_{o1,2}}{\partial x} = \pm\gamma\frac{(I_{e1}I_{e2})^{1/2}}{I_0}(I_{e1,2})^{1/2} \times\cos(2\Psi_{e1,2} - \Psi_{e2,1} - \Psi_{o1,2} + \Delta\alpha x), \tag{18}$$

and

$$\frac{\partial \Psi_{e1,2}}{\partial x}(I_{e1,2})^{1/2} = \mp\gamma\frac{(I_{e1}I_{e2})^{1/2}}{I_0}(I_{o1,2})^{1/2} \times\sin(\Psi_{o1,2} - 2\Psi_{e1,2} + \Psi_{e2,1} - \Delta\alpha x)$$
$$\frac{\partial \Psi_{o1,2}}{\partial x}(I_{o1,2})^{1/2} = \pm\gamma\frac{(I_{e1}I_{e2})^{1/2}}{I_0}(I_{e1,2})^{1/2} \times\sin(2\Psi_{e1,2} - \Psi_{e2,1} - \Psi_{o1,2} + \Delta\alpha x). \tag{19}$$

Since it is hard to obtain the analytic solutions of (18) and (19), we make an assumption to simplify (18) and (19). We assume that the phase relation in (17) still holds under the condition of large modulation. After substituting (17) into (18) and using the conservation laws as expressed in (7), we can obtain the solutions easily as

$$I_{e1,2}(x) = \frac{I_{e1,2}(0)}{1+\left[\gamma m\frac{\sin(\Delta\alpha x/2)}{\Delta\alpha/2}\right]^2}$$
$$I_{o1,2}(x) = \frac{I_{e1,2}(0)}{1+\left[\gamma m\frac{\sin(\Delta\alpha x/2)}{\Delta\alpha/2}\right]^{-2}}. \tag{20}$$

It shows that (20) will reduce to (8) when $\Delta\alpha = 0$, i.e. the phase-match condition, and will reduce to (16) when $m \ll 1$, i.e. the small-modulation approximation. From (20), the diffraction efficiency oscillates as the quantity of phase mismatch increases. The zero diffraction efficiency occurs when

$$\Delta\alpha x/2 = N\pi, \tag{21}$$

where N is an integer. Equation (21) would be helpful for estimating the Bragg constraint of the ASD when $N = 1$. It will be discussed in Sect. 4.

In deriving (20), we assume that the phase relation under small modulation as expressed in (17) still holds for large modulation. To judge the reliability of the assumption, we substitute (17) into (19) and obtain the equation of the phase relations as

$$\frac{\partial}{\partial x}(2\Psi_{e1,2} - \Psi_{2,1} - \Psi_{o1,2}) = \frac{\Delta\alpha}{2}\left(\frac{3C^2-1}{C^2+1}\right), \tag{22}$$

where $C = \gamma m\frac{\sin(\Delta\alpha x/2)}{\Delta\alpha/2}$. According to (17), the right-hand side of (22) should be $-\Delta\alpha/2$, i.e. C must be zero. However, $C = 0$ only occurs when the condition shown in (21) is satisfied. This means that we can exactly predict the zero diffraction points under large modulation with (21) but there is a phase error in the other regions. This will induce a slight deviation of the diffraction intensity between the calculation with use of (20) and the numerical calculation. The phase error affects the prediction of the diffraction efficiency for a slight deviation except the zero diffraction points. Therefore, (20) can be regarded as a common solution describing the ASD under Bragg mismatch in general condition. The value of C decreases as the phase mismatch increases or the coupling strength decreases. The error will be discussed experimentally in the next section.

3 Experiment and discussion

The experimental setup is shown in Fig. 3. We used an argon ion laser as the light source. The wavelength was 514.5 nm. A plane wave and a converging wave with extraordinary polarization were incident on the crystal. In the experiment, four $BaTiO_3$ crystals with different thickness were used. The angle between the plane wave and the central direction of the converging wave satisfied the Bragg condition. Thus, the light deviated from the central direction of the converging wave

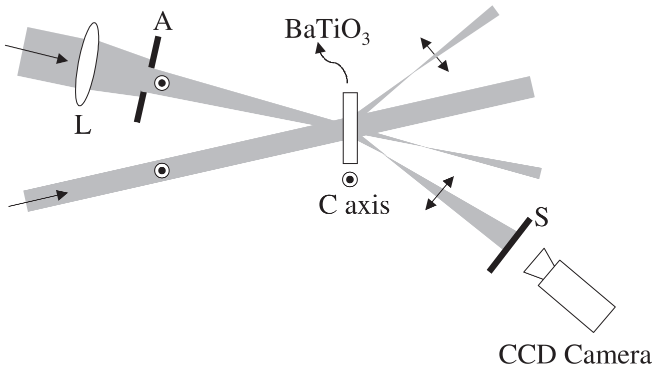

Fig. 3. Experimental setup. L, lens; A, aperture; S, output screen

was under Bragg mismatch. It should be noted that the converging wave was focused behind the crystal, so the beams with different orientation of the converging wave were independent of each other. Thus, although there were many gratings with different wave vectors generated in the crystal, every beam with different direction read the corresponding grating only. Figure 4 shows the schematic diagram of the incident condition in k space. The bold solid lines denote the plane wave and the axial direction of the converging wave, respectively. The bold dashed line denotes the converging light deviated from the Bragg angle with angle of $\Delta\theta$. In our experiments, the external half angle of the converging light was about 1°. The range of the converging light covered several zero diffraction points. Using (3), (12), and the geometrical relation

$$3n_\mathrm{e}\sin(\theta_\mathrm{i}+\Delta\theta/2)=n_\mathrm{o}\sin(\theta_\mathrm{d}+\Delta\varphi-\Delta\theta/2), \tag{23}$$

we can calculate the quantity of phase mismatch as a function of angle deviation expressed as

$$\begin{aligned}\Delta\alpha &= \frac{4\pi}{\lambda}n_\mathrm{e}\sin\theta_\mathrm{i}\Delta\varphi\\ \Delta\varphi &= 2\Delta\theta,\end{aligned} \tag{24}$$

where $\Delta\varphi$ is the deviation of the diffraction angle from the Bragg angle θ_d in the crystal. The diffraction pattern captured by a CCD camera is shown in Fig. 5. Obviously, the oscillation of diffracted light intensity with respect to the angle deviation is same with the prediction of (20). We measured the angle deviation between two adjacent zero points in four crystals of different thickness. The measured results and the theoretical predictions using (24) are shown in Fig. 6. The results fit the theory fairly well. Figure 7 shows the experimental measurement for the normalized diffraction intensity with respect to the deviated angle and its corresponding calculation with the use of (20) and the numerical simulation with the use of (18) and (19). Figure 7a shows the result when the modulation depth is 0.23. The difference between the curve with (20) and that with (18) and (19) is small and is caused by the phase error in (20). Both calculations can predict the experiment observation. When the modulation depth is as small as 0.07, both calculations can accurately predict the experimental results, as shown in Fig. 7b. It should be addressed that the experimental data in these two figures are obtained through a smooth process to get rid of the unwanted

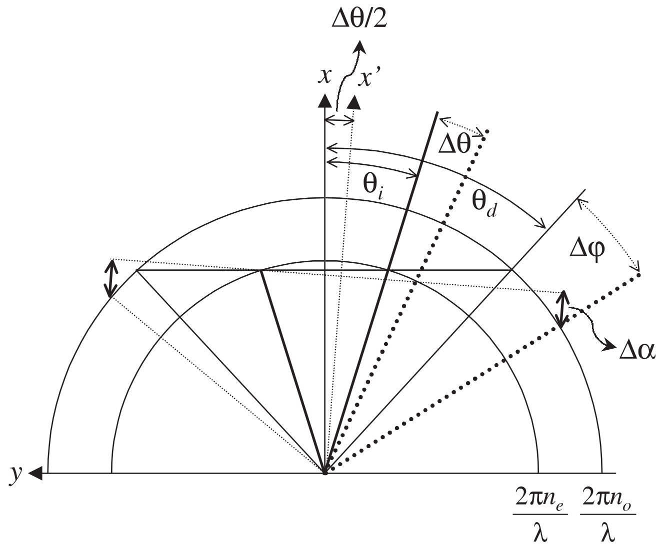

Fig. 4. Schematic diagram of the setup in k space. The *bold solid lines* denote the central light of the converging wave and the plane wave under Bragg condition. The *bold dashed line* denotes the converging light deviated from the Bragg angle

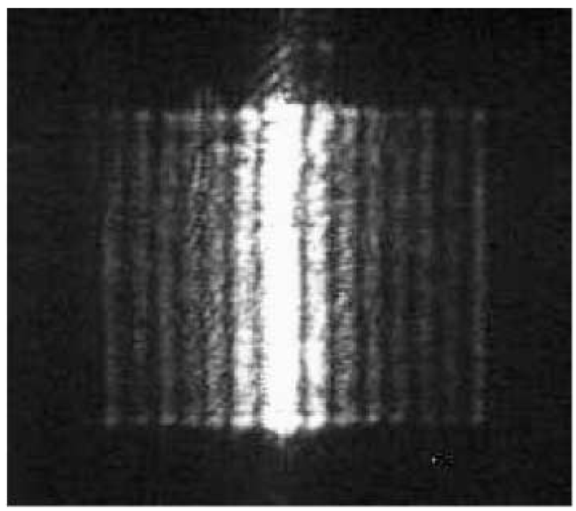

Fig. 5. Diffracted pattern in the experiment as shown in Fig. 4. The center of the pattern corresponds to the Bragg match

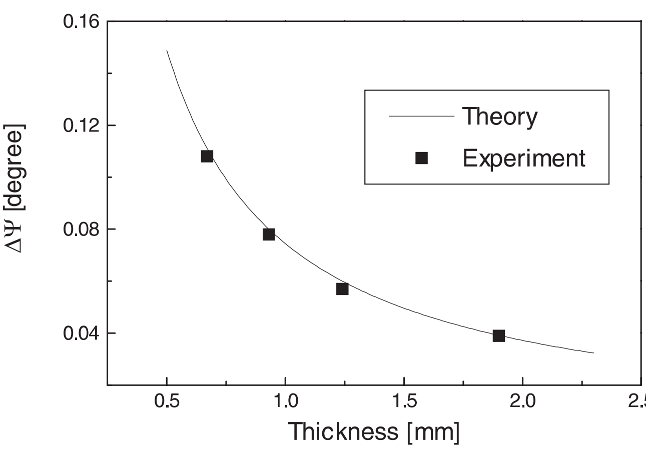

Fig. 6. Angle deviation between two adjacent zero points with respect to the thickness of the crystal

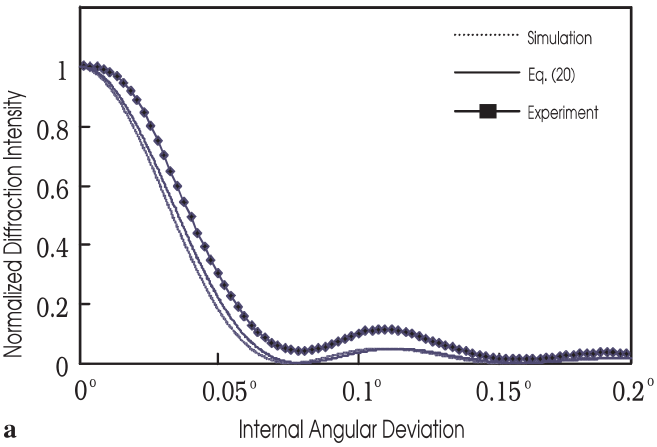

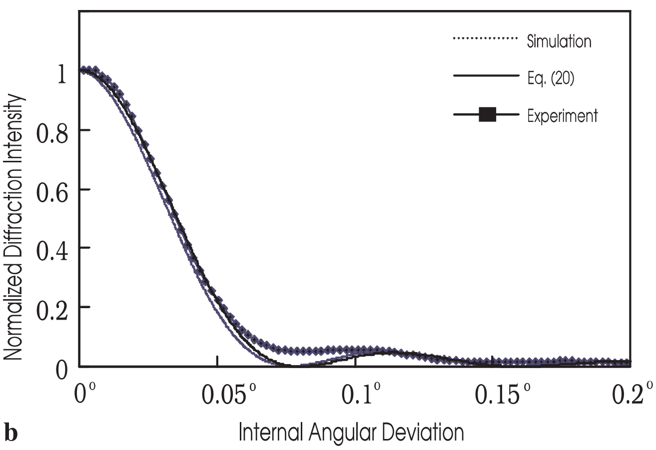

Fig. 7a,b. Normalized diffraction intensity with respect to the internal angular deviation from the Bragg angle. **a** $m = 0.23$, **b** $m = 0.07$

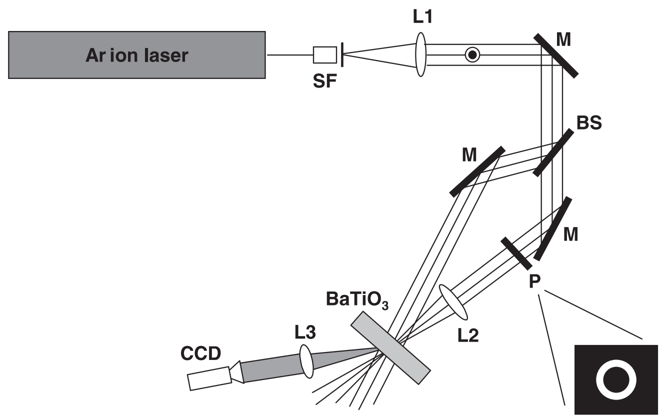

Fig. 8. Experimental setup of the symmetry filter based on the ASD. SF, spatial filter; L, lens; PBS, polarized beam splitter; M, mirror; P, input pattern; HWP, half-wave plate

noise. These experimental results indicate that (20) can usefully describe the ASD under Bragg mismatch without taking a complicated numerical simulation with the use of (18) and (19).

4 Shift tolerance of a spatial filter with use of the ASD

The ASD in $BaTiO_3$ crystal has been applied to spatial filtering such as central symmetry filter [12]. According to the phase relation in (9), when one of the writing lights is a plane wave and the other is the Fourier transform of an image, the Fourier transform of the diffracted output is the autoconvolution of the image. If the image is central symmetric, there will be a peak centered at the autoconvolution pattern. Thus, a symmetry filtering can be performed by examining the central peak intensity. The schematic diagram of the symmetry filter based on the ASD is shown in Fig. 8. The test image (a circle) is placed on one of the two incident beams and is Fourier transformed onto the crystal, then a CCD camera is used to monitor the intensity of the output pattern. Figure 9 shows the diffracted autoconvolution pattern of a circle shown in Fig. 8 with different crystal thickness. Figure 9a shows the output pattern, where a crystal of thickness 2.5 mm is used. The slit-like pattern is caused by the Bragg constraint. When a thin crystal of thickness 670 μm is used, the Bragg constraint is not so significant and almost the full autoconvolution pattern can be observed. These results coincide with our theory.

From (21), under the condition of Bragg mismatch, the first zero diffraction point locates at

$$\Delta\alpha = \frac{2\pi}{x}, \tag{25}$$

where x is the crystal thickness. According to (24), we can rewrite (25) as

$$\Delta\theta = \frac{\lambda}{4n_e \sin\theta_i x}, \tag{26}$$

where $\Delta\theta$ is the internal angular deviation of the incident light deviated from the Bragg angle. Applying Snell's law, we

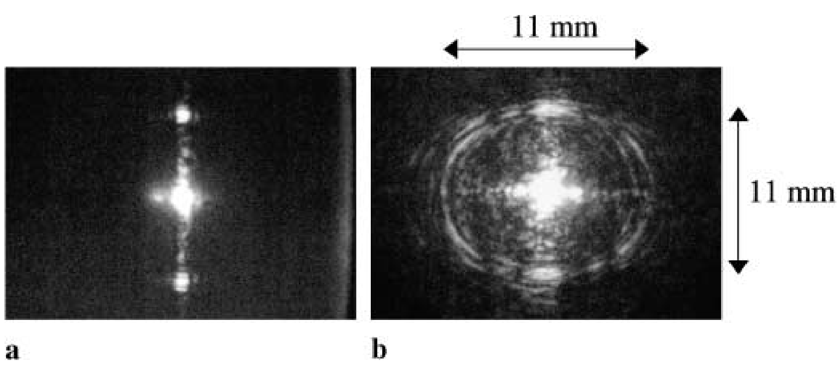

Fig. 9a,b. Autoconvolution of a circle. **a** The thickness of the thick crystal is 2.5 mm. **b** The thickness of a thin crystal is 670 μm

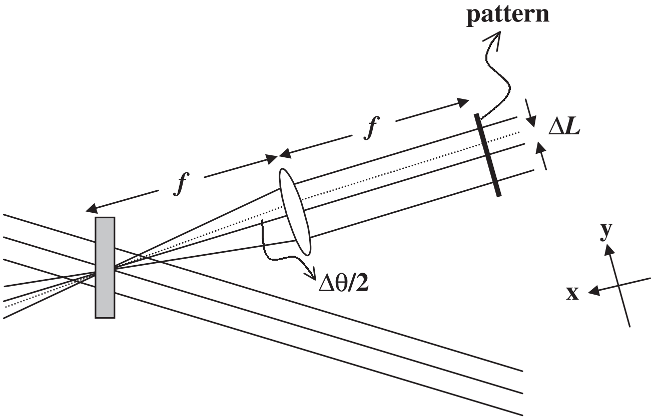

Fig. 10. Shift tolerance caused by the displacement of the input pattern 12

can express the external angular deviation of the incident light as

$$\Delta\theta_o \approx \frac{\lambda}{4\sin\theta_i x}. \tag{27}$$

Consequently, in Fig. 10, we know that the central peak of the autoconvolution pattern decays to zero when the central incident angle of the pattern deviates from the Bragg angle over $(\lambda/4\sin\theta_i x)$. Now we can define that the shift tolerance in y direction is $(\Delta\theta_o/2)$, so the full tolerance is $\Delta\theta_o$. From Fig. 8, the shift tolerance of the pattern in the y direction can be expressed as

$$\Delta L = f\Delta\theta_o \approx \frac{f\lambda}{4\sin\theta_i x}, \tag{28}$$

where f is the focal length of the lens L2 shown in Fig. 8. If $\lambda = 514.5$ nm, $n_e = 2.424$, and $n_o = 2.488$, the shift tolerance of the pattern in a $BaTiO_3$ is obtained as

$$\Delta L = 0.001573\frac{f}{x}, \tag{29}$$

where ΔL is expressed in millimeters. From (29), the shift tolerance is proportional to the focal length and is inversely proportional to the crystal thickness. In addition, the autoconvolution output is insensitive to shifting in the z direction owing to the Bragg degeneracy [15, 17].

5 Conclusion

The property of anisotropic self-diffraction under Bragg mismatch has been demonstrated. A solution shown in (20) can satisfactorily describe the ASD, and the theoretical prediction coincides with the experimental measurements. The angle between two adjacent zero points is inversely proportional to the thickness of the crystal. Accordingly, a simple equation for estimating the shift tolerance of an optical spatial filter based on the ASD is proposed. The corresponding experiments show a similar result. Consequently, the thickness of the crystal is one of the most important factors of the ASD applied to optical information processing.

Acknowledgements. The authors would like to appreciate N.V. Kukhtarev for his helpful discussions. This study is supported by the National Science Council of the Republic of China.

References

1. J.-P. Huignard, P. Gunter: *Photorefractive Materials and Their Applications: I. Fundamental Phenomena* (Springer, New York 1988)
2. J.-P. Huignard, P. Gunter: *Photorefractive Materials and Their Applications: II. Applications* (Springer, New York 1989)
3. Y. Fainman, E. Klancnik, S.H. Lee: Opt. Eng. **25**, 228 (1986)
4. J.H. Hong, P. Yeh, D. Psaltis, D. Brady: Opt. Lett. **16**, 1520 (1991)
5. C.C. Sun, M.W. Chang, K.Y. Hsu: Opt. Lett. **18**, 655 (1993)
6. C.C. Sun, M.W. Chang, K.Y. Hsu: Opt. Commun. **119**, 597 (1995)
7. H. Kogelnik: Bell Syst. Tech. J. **48**, 2909 (1969)
8. N.V. Kukhtarev, E. Krätzig, H.C. Kulich, R.A. Rupp: Appl. Phys. B **35**, 17 (1984)
9. C.C. Sun, M.W. Chang, K.Y. Hsu: Appl. Opt. **33**, 4501 (1994)
10. C.C. Sun, M.W. Chang, K.Y. Hsu: Int. J. Optoelectron. **11**, 413 (1997)
11. C.C. Sun, B. Wang, J.Y. Chang: Appl. Opt. **37**, 8247 (1998)
12. C.C. Sun, B. Wang, W.C. Su, A.E.T. Chiou, J.Y. Chang: Appl. Opt. **38**, 3720 (1999)
13. A. Yariv, P. Yeh: *Optical Waves in Crystals* (Wiley, New York 1984)
14. C.C. Sun, M.W. Chang, K.Y. Hsu: Int. J. Optoelectron. **11**, 413 (1997)
15. R.M. Pierce, R.S. Cudney: Opt. Lett. **17**, 784 (1992)
16. C.C. Sun, M.S. Tsau, W.C. Su, B. Wang, A.E.T. Chiou: Appl. Opt. **38**, 4316 (1999)
17. C. Gu, J. Hong, S. Campbell: Opt. Commun. **88**, 309 (1992)